A EUROPEAN JOURNAL OF CHEMICAL BIOLOGY

CHEMBIOCHEM

SYNTHETIC BIOLOGY & BIO-NANOTECHNOLOGY

Accepted Article

Title: R-ω-Transaminase Covalently Linking to D-Amino Acid Oxidase Through Protein Splicing to Enhance Enzymatic Catalysis of Transamination of Amines

Authors: Wei Feng, Kun Du, Rong Li, and Dongrui Zhang

To be cited as: *ChemBioChem* 10.1002/cbic.201800646

Link to VoR: http://dx.doi.org/10.1002/cbic.201800646

A Journal of ChemPubSoc Europe

WILEY-VCH www.chembiochem.org

R-ω-Transaminase Covalently Linking to D-Amino Acid Oxidase Through Protein Splicing to Enhance Enzymatic Catalysis of Transamination of Amines

Kun Du[†], Rong Li[†], Dongrui Zhang, Wei Feng[*]

R-ω-Transaminases (RTA) catalyze the conversion of (*R*)-amines (e.g. (*R*)-1-phenylethylamine) to corresponding ketones (e.g. acetylbenzene), by transferring an amino group from an amino donor (e.g. (*R*)-1-phenylethylamine) onto an amino acceptor (e.g. pyruvate), resulting in a co-product (e.g. D-alanine). D-alanine can be deaminated back to pyruvate by D-amino acid oxidase (DAAO). Herein, through the vivo subunit splicing, the N-terminus of the RTA subunit (RTA^S) was specifically ligated to the C-terminus of the DAAO subunit ($DAAO^S$) with native peptide bonds (RTA&DAAO). RTA^S is in close proximity to $DAAO^S$ at a molecular distance. Thus the transferring of pyruvate and D-alanine between RTA and DAAO can be directional and efficient. The pyruvate→D-alanine→pyruvate cycles are efficiently formed, promoting the transamination reaction forward. In an in vitro non-covalent approach, through the coiled-coil association, the N-terminus of RTA^S was specifically associated with the C-terminus of $DAAO^S$ (RTA#DAAO). In addition, the mixed two enzymes RTA+DAAO was also studied. RTA&DAAO has a shorter distance between the paired subunits RTA^S–$DAAO^S$ than RTA#DAAO, and the number of the paired subunits is higher than that of RTA#DAAO. While RTA+DAAO cannot form the paired subunits. For transamination of the amines, RTA&DAAO exhibited a higher catalysis efficiency

[*] Department of Biochemical Engineering, Beijing University of Chemical Technology, Beijing, China. E-mail: fengwei@mail.buct.edu.cn
[†] These authors contributed equally to this work

than RTA#DAAO, and a much higher catalysis efficiency than RTA+DAAO.

Keywords: *R*-ω-Transaminase; D-amino acid oxidase; protein splicing; pyruvate

Introduction

Chiral amines are important chemicals for the synthesis of pharmaceuticals.[1,2,3] ω-Transaminases (ω-TAs) are multimeric enzymes[4] and have been investigated for the preparation of chiral amines.[5] The amines in optically pure form can be used for the synthesis of biologically active compounds.[6] (*R*)-enantioselective transaminases (RTAs) have been used for the kinetic resolution of racemic amines.[7] RTAs catalyze the conversion of (*R*)-amines (e.g. (*R*)-1-phenylethylamine) to corresponding ketones (e.g. acetylbenzene), by transferring an amino group from an amino donor (e.g. (*R*)-1-phenylethylamine) onto an amino acceptor (e.g. pyruvate), resulting in a co-product (e.g. D-alanine). Pyruvate has been extensively used as amino acceptor in RTA catalyzing processes.[8] Catalytic amount of pyruvate favors the transamination reaction and facilitates subsequent purification.[8] This requires the recycling of pyruvate *in situ*. D-amino acid oxidases (DAAOs) are dimeric enzymes that catalyze a D-amino acid substrate into α-keto acid.[9] D-amino acid oxidase was used together with (*R*)-enantioselective transaminase,[10] catalyzing the deamination of D-alanine back to pyruvate, achieving the recycling of pyruvate *in situ*.

However, for the conversion of some amines, for example (R)-phenethylamine, (R)-1-aminoindan, and furfurylamine, we found that the combined two enzymes RTA+DAAO achieved a very low substrate conversion. It is speculated that D-alanine and pyruvate were transferred between RTA and DAAO with a low efficiency. Spatially arranging RTA and DAAO at a short distance is a solution to improving the transport efficiency. It is ideal that the distance between RTA and DAAO is at a molecular distance. This requires the RTA and DAAO subunits being arranged in a one-by-one

fashion. Gene fusion can be a solution to linking two enzymes.[11] We have fused the genes of RTA and DAAO, and the fusion gene was expressed in *Escherichia coli*. However, the expressed fusion enzyme did not exhibit any enzymatic activity. Possibly, it is because the multimeric enzymes RTA and DAAO having large molecular weights, the fusion enzyme did not have a correct folding in the *Escherichia coli* cell.

Previously, we have specifically ligated two multimeric enzymes with native peptides through intein-mediated in vivo subunit splicing.[12,13] Herein, we extend the in vivo subunit splicing methodology to specifically ligate demeric RTA and dimeric DAAO, in order to investigate the importance of efficiently forming the pyruvate→ D-alanine→ pyruvate cycles between RTA and DAAO for transamination reaction. The C-terminal domain of the split NpuDnaE intein [14] is fused to the N-terminus of the RTA subunit. The N-terminal domain of the split NpuDnaE intein is fused to the C-terminus of the DAAO subunit. Through the intein-mediated subunit splicing,[12] the N-terminus of the RTA subunit is specifically ligated to the C-terminus of the DAAO subunit with native peptides, as illustrated in Figure 1. Thus, the RTA and DAAO subunits can be spatially arranged in a one-by-one fashion at a molecular distance. For comparison, an in vitro non-covalent approach is investigated. An arginine-rich leucine zipper (Z_R) [15] is fused to the N-terminus of RTA subunit, and a glutamic acid-rich leucine zipper (Z_E) [15] is fused to the C-terminus of DAAO subunits. The N-terminus of RTA subunit is associated with the C-terminus of DAAO subunit through the coiled-coil association of Z_E and Z_R in vitro, resulting in an association product RTA#DAAO, as illustrated in Figure 2. The two-enzyme systems have been evaluated for the conversion of amines. Their stability is also investigated.

Results

Two-enzyme system RTA&DAAO though in vivo subunit splicing

R-ω-Transaminase (RTA) and D-Amino oxidase (DAAO) are dimeric enzymes. The N-terminal domain of the split NpuDnaE intein (Int^N) [14] was fused to the C-terminus of the DAAO subunit. The C-terminal domain of the split NpuDnaE intein (Int^C)[14] was fused to the N-terminus of the RTA subunit (supplementary Figure S1). A rigid α-helical linker (EPPPPLPPPPLPPPPEPPPP) between Int^C and the RTA subunit and between Int^N and the DAAO subunit are required, in order to reduce the steric hindrance for the splicing of multimeric enzymes.

The splicing product RTA&DAAO was purified through Ni Sepharose beads and ultrafiltration fractionation. Thus those RTA and DAAO, that were not involved in the splicing reactions, were separated from the splicing product RTA&DAAO. The purified RTA&DAAO was analyzed by sodium dodecyl sulfate polyacrylamide gel electrophoresis (SDS-PAGE) (Figure 3a). The top band is ascribed to the RTA^S-$DAAO^S$ subunit. It is the key subunit in RTA&DAAO. Appearance of the RTA^S-$DAAO^S$ subunit band confirmed the ligation of the RTA and DAAO subunits through the in vivo posttranslational subunit splicing. The bands for Int^C-link-RTA and Int^N-link-DAAO are ascribed to those subunits that did not take part in the subunit splicing reaction, but they were associated with the RTA^S-$DAAO^S$ subunit in RTA&DAAO (Figure 3c). In comparison to the RTA (supplementary Figure S2a) and DAAO (supplementary Figure S2b) subunits, the Int^C-link-RTA and Int^N-link-DAAO subunits exhibited larger molecular weights due to being fused to the C- and N-terminal domains of the split intein, respectively.

RTA&DAAO was analyzed by MALDI-TOF-MS in order to determine its molecular weight. However, the measured data are not reliable, possibly because the RTA&DAAO fractions have large molecular weights. RTA&DAAO was analyzed by blue native polyacrylamide gel electrophoresis (BN-PAGE). BN-PAGE has been often

used for identification of proteins from multiprotein complexes.[16] The BN-PAGE of RTA&DAAO is illustrated in Figure 3b. Six bands appeared for RTA&DAAO. Lane M is for Marker proteins. Based on lane M, the relationship of the electrophoretic mobility of marker proteins versus the molecular weight was obtained, as shown in supplementary Figure S3a. The function shown in Figure S3a was used to estimate the apparent molecular weights (AMWs) corresponding to the six bands, by comparing the electrophoretic mobility of the bands with that of marker proteins. The AMWs of the bands I, II, III, IV, V, and VI were determined to be 1152, 710, 581, 522, 399, and 268 kDa, respectively. Then we searched the ligation modes with theoretical molecular weights (TMWs) being in accordance with these AMWs. Based on the molecular weights of intein and the Int^C-link-RTA and DAAO-link-Int^N subunits, the TMWs of the possible ligation modes were predicated. Supplementary Table S1 lists those ligation modes with TMWs being in accordance with the AMWs of the six bands. The ligation modes were finally determined to be, RTA~DAAO~RTA~DAAO~RTA~DAAO~RTA~DAAO~RTA~DAAO~RTA~DAAO~RTA~DAAO~RTA (band I); RTA~DAAO~RTA~DAAO~RTA~DAAO~RTA~DAAO~RTA (band II); DAAO~RTA~DAAO~RTA~DAAO~RTA~DAAO (band III); RTA~DAAO~RTA~DAAO~RTA~DAAO~RTA (band IV); RTA~DAAO~RTA~DAAO~RTA (band V); DAAO~RTA~DAAO (band VI). Figure 3c schematically illustrates the ligation modes corresponding to the six bands. The RTA^S-$DAAO^S$ subunit (as illustrated by  in Figure 3c) is formed by the hetrosubunit ligation with a peptide bond through the subunit splicing, and it is the key subunit in the RTA&DAAO fractions. Those RTA and DAAO subunits that are not involved in the subunit splicing are associated with the RTA^S-$DAAO^S$ subunit, as illustrated in Figure 1. The relative abundances of the six bands were estimated based on the intensity, they are 10.1%, 11.7%, 0.5%, 1.0%, 7.5%,

and 69.2% for bands I, II, III, IV, V, and VI, respectively. The averaged apparent molecular weight of RTA&DAAO was estimated to be 408 kDa

Two-enzyme system RTA#DAAO though in vitro subunit association

In an in vitro non-covalent approach, an arginine-rich leucine zipper (Z_R) was fused to the N-terminus of the RTA subunit, and a glutamic acid-rich leucine zipper (Z_E) was fused to the C-terminus of the DAAO subunit (supplementary Figure S4). The rigid α-helical linker (EPPPPLPPPPLPPPPEPPPP) between Z_R and the RTA subunit and between Z_E and the DAAO subunit are required in order to promote the coiled-coil association of Z_R and Z_E. The purified DAAO-Z_E and RTA-Z_R were analyzed by SDS-PAGE (supplementary Figure S5). The N-terminus of the RTA subunit was associated with the C-terminus of the DAAO subunit through the coiled-coil association of Z_E and Z_R, resulting in the association product RTA#DAAO, and the RTA^S=$DAAO^S$ subunit (as illustrated in Figure 2) is the key subunit. The BN-PAGE analysis (Figure 4a) revealed that RTA#DAAO comprises three fractions. The apparent molecular weights (AMWs) corresponding to the three bands were estimated by comparing the electrophoretic mobility of the bands with that of marker proteins (supplementary Figure S3b). The AMWs of the bands I, II, and III are 560, 419, and 289 kDa, respectively. Then we searched the association modes with theoretical molecular weights (TMWs) being in accordance with these AMWs. Based on the molecular weights of the RTA-Z_R and DAAO-Z_E subunits, the theoretical molecular weights of possible association modes were predicated. Supplementary Table S2 lists those association modes with TMWs being in accordance with the AMWs of the three bands. The association modes were finally determined to be RTA≈DAAO≈RTA≈DAAO≈RTA≈DAAO≈RTA (band I); RTA≈DAAO≈RTA≈DAAO≈RTA (band II); DAAO≈RTA≈DAAO (band III). (Figure 4b). The relative

abundances of the bands were estimated based on the intensity, they are 5.4% for band I, 16.3% for band II, and 78.3% for band III. The apparent molecular weight of RTA#DAAO was estimated to be 309 k.

Schematic presentations in Figures 3c and 4b illustrate that the RTA^{S}-$DAAO^{S}$ subunit is the key subunit in the splicing product RTA&DAAO and the RTA^{S}=$DAAO^{S}$ subunit is the key subunit in the association product RTA#DAAO. Based on the average AMWs of RTA&DAAO and RTA#DAAO and the MWs of the RTA^{S}-$DAAO^{S}$ and RTA^{S}=$DAAO^{S}$ subunits, the number of the RTA^{S}-$DAAO^{S}$ subunit in RTA&DAAO is 23.1% higher than that of the RTA^{S}=$DAAO^{S}$ subunit in RTA#DAAO. It means that RTA&DAAO comprises more paired subunits than RTA#DAAO.

Stability of RTA&DAAO and RTA#DAAO

The stability of multimeric enzymes is also of significant concern. Multimeric enzymes may be inactivated due to the dissociation of the enzyme subunits.[17,18] For multimeric enzymes, the subunit–subunit interactions maintain the quaternary structures. However, the interactions are reduced under certain experimental conditions, leading to decreasing the enzymatic activity.[19] The moderate-to-low stability of multimeric enzymes hinders their applications at industrial scale. The multimeric enzymes RTA and DAAO also face the same concern of stability.

Activity assay has shown that RTA&DAAO and RTA#DAAO can catalyze transamination and deamination, indicating that the enzymatic activities of RTA and DAAO have been retained by RTA&DAAO and RTA#DAAO. It is implied that after the in vivo subunit splicing and in vitro non-covalent association, the original quaternary structures of RTA and DAAO have been preserved. Circular dichroism (CD) spectra were measured to monitor the change of the secondary structures of the enzymes after the in vivo subunit splicing and the in vitro subunit association. Figure 5 shows

the CD spectra for RTA&DAAO, RTA#DAAO, and the mixed enzymes RTA+DAAO (control). The intensity difference between three CD spectra are very small. Figure 5 demonstrates that the in vivo subunit splicing and the in vitro non-covalent association had little effect on the secondary structures of the enzymes.

Fluorescence spectra were measured for RTA&DAAO, RTA#DAAO, and RTA+DAAO using urea as denaturing agent. To investigate the conformational change upon interfering by urea, the intrinsic fluorescence of the two-enzyme systems was quenched by acrylamide. The fluorescence spectra with excitation of 295 nm are shown Figure 6a, 6b, and 6c. The concentration-dependence quenching was evaluated by the Stern-Volmer equation $F_0/F=1+ K_{SV}[C]$,[20] where F_0 and F are the fluorescence intensities in the absence and presence of acrylamide, respectively. [C] is the acrylamide concentration. The Stern-Volmer quenching constant K_{SV} was compared to investigate the conformational change.[20] A larger K_{SV} value is obtained when the protein has a larger conformational change. Figure 6d shows the Stern-Volmer plots for the two-enzyme systems. The K_{SV} value for RTA&DAAO at the urea concentration (4 M) is 7.61, which is smaller than 9.12 for RTA#DAAO and 10.29 for RTA+DAAO. Both RTA&DAAO and RTA#DAAO are more stable than the mixed enzymes RTA+DAAO (control). In comparison to RTA&DAAO, RTA#DAAO is more inclined to expose the tryptophan residues when interfered by urea. The association product RTA#DAAO has a lower stability than the splicing product RTA&DAAO upon the urea denaturation. RTA&DAAO resulted from the covalent bonding of the RTA and DAAO subunits, in contrast to RTA#DAAO obtained from the coiled-coil association. The BN-PAGE analysis based on Figures 3c and 4b show that, the number of the RTA^S-$DAAO^S$ subunit in RTA&DAAO is 23.1% higher than that of the RTA^S=$DAAO^S$ subunit in RTA#DAAO (per gram of enzymes). This led to a lower mobility of the

subunits in RTA&DAAO, which may become more rigid than RTA#DAAO.

Enzymatic activity

The enzymatic activity for catalyzing the D-alanine deamination reaction by DAAO and RTA&DAAO was investigated, in order to investigate the effect of the hetrosubunit ligation on the catalysis efficiency. In the deamination reaction, D-alanine is converted to pyruvate. 2,4-Dinitrophenylhydrazine (DNPH) can react with pyruvate to produce a coloured product.[21] It was added to the reaction systems for the qualitative comparison of enzymatic activity. Both the solutions of DAAO and RTA&DAAO exhibited a colour in yellow (Figure S6a), there is no significant difference in the colour intensity between the DAAO and RTA&DAAO solutions. Figure S6 indicated that RTA&DAAO exhibited almost the same capability with DAAO for catalyzing the deamination of D-alanine. Furthermore, a quantitative comparison was performed by studying the enzyme kinetics. The kinetics of RTA&DAAO was compared with that of DAAO. Figure S6b shows the plots of the initial rate of reaction versus the concentration of D-alanine. The kinetics parameters were obtained by regressing the data using the Michaelis-Menten kinetics equation. RTA&DAAO exhibited a *Km* value 15.88 mM, which is comparable to that 15.37 mM by DAAO, indicating that the effect of the ligation of hetrosubunits on the affinity towards the substrate is very small. RTA&DAAO exhibited a *Kcat* value of 1115.5 min^{-1}, in comparison to the *Kcat* value of 1155.8 min^{-1} by DAAO, indicating that RTA&DAAO exhibited a turnover number being comparable with that by DAAO. The *Kcat/Km* ratio is a measure of catalysis efficiency.[22] The *Kcat/Km* ratio of RTA&DAAO is 70.3 mM^{-1} min^{-1}, which is 93.4% of that of DAAO 75.2 mM^{-1} min^{-1}. It is indicated that the ligation of hetrosubunits has a very small effect on the catalysis efficiency of DAAO.

In *R*-ω-transaminase catalyzing reactions, amine conversion can be carried out by

using pyruvate as an amine acceptor, and D-alanine is the resulting co-product. It is better to maintain pyruvate at a low concentration in order to facilitate subsequent product purification.[8] On the other hand, *in situ* removal of D-alanine eliminates the by-product inhibitory effect. In the enzymatic activity assay, a small amount of pyruvate (0.5 mM) was used, which is tenth of that of (*R*)-amines (5 mM). The transamination of amines was catalyzed under RTA&DAAO, RTA#DAAO, and RTA+DAAO. Figure 8a shows the profile of furfurylamine conversion versus reaction time. The control reaction using RTA+DAAO achieved a conversion of 11.1% after 6 h reaction, and 18.5% of furfurylamine was converted under the catalysis of RTA#DAAO. For these two-enzyme systems, after 5 h reactions, the conversions reached a plateau. In contrast, RTA&DAAO achieved a furfurylamine conversion of 56.3% after 6 h reaction, much higher than the conversions achieved by RTA#DAAO and RTA+DAAO. Figure 7a shows that RTA&DAAO exhibited much higher catalysis efficiency than RTA#DAAO and RTA+DAAO for the conversion of furfurylamine. Figure 7b shows the result of the conversion of (R)-2-aminooctane. The conversions were 77.9%, 58.4, and 32.3% after 6 h reactions for RTA&DAAO, RTA#DAAO, and RTA+DAAO, respectively, indicating the advantage of RTA&DAAO over RTA#DAAO and RTA+DAAO. For the conversions of phenethylamine (Figure 7c), RTA&DAAO exhibited a higher catalysis efficiency than RTA#DAAO, and much higher efficiency than RTA+DAAO (control).

The three two-enzyme systems were used for the resolution of α-methylbenzylamine. The conversion and enantiomeric excess are shown in Figure S7, closed symbols showing enantiomeric excess and open symbols presenting conversion. The results of conversion and enantiomeric excess show that the splicing product RTA&DAAO needed 80 min to reach 50% conversion yielding the S-product (99% e.e), in contrast to 120 min required by RTA#DAAO and 180 min needed by RTA+DAAO. The results demonstrated the splicing product RTA&DAAO exhibited a

higher catalytic efficiency than RTA#DAAO and RTA+DAAO for the kinetic resolution of high concentration of racemic amine.

Discussion

Under the catalysis of the two-enzyme systems, the by-product D-alanine can be deaminated back to pyruvate under the catalysis of DAAO, achieving the recycling of pyruvate. In a separate experiment, we performed the RTA catalysis by using an excess amount of pyruvate (6 mM) in comparison to amines (5 mM), the catalysis efficiency was lower than that under the catalysis of RTA together with DAAO with a catalytic amount of pyruvate (0.5 mM). It is ascribed to that the co-substrate pyruvate has an inhibitory effect on the transamination reaction.[8,10] Hence the recycling of pyruvate is necessary for the transamination reaction. For the mixed two enzymes RTA+DAAO, there are no specific interactions between the two enzymes. In the period of reaction time, the enzyme molecules moved randomly in the reaction solution, and the pairing of RTA and DAAO might be occasionally occurred due to the enzyme motion. However, such kind of enzyme pairing is instantaneous and cannot be lasted for a long time due to the lack of specific interaction. As a result, the diffusion and transferring of D-alanine and pyruvate between RTA and DAAO cannot be directional, and the pyruvate→D-alanine→pyruvate cycle cannot be formed for the mixed two enzymes RTA+DAAO. In contrast, RTA&DAAO was obtained via in vivo splicing of hetrosubunits (a covalent approach to linking the hertrosubunits), RTA#DAAO was a result of association of hetrosubunits (a non-covalent approach to associate the hertrosubunits). Both RTA&DAAO and RTA#DAAO achieved the pairing of the RTA and DAAO subunits, as illustrated in Figures 1 and 2. The distance travelled by D-alanine and pyruvate between RTA to DAAO is short due to the subunit pairing, facilitating the transfer of D-alanine and pyruvate. The diffusion and transferring of D-alanine and pyruvate are

directional. In RTA&DAAO, the paired subunits RTA^S-$DAAO^S$ were formed by the direct ligation of two terminal linkers as illustrated in Figure 1 and Figure 8a. While in RTA#DAAO, the paired subunits RTA^S=$DAAO^S$ were formed by the association interaction of two terminal peptides Z_R and Z_E as shown in Figure 2 and Figure 8b. Using the software Discovery Studio 4.5, the length of the linker is 3.3 nm, and the lengths of the peptides Z_R and Z_E are 7.9 and 7.2 nm, respectively. The largest distance between the paired subunits of RTA^S and $DAAO^S$ in RTA&DAAO is 6.6 nm (3.3+3.3 nm, Figure 8a). The smallest distance between the paired subunits of RTA^S and $DAAO^S$ in RTA#DAAO is 14.5 nm {6.6 nm + 7.9 nm (the smallest length of associated peptides, Z_R and Z_E being completely overlapped)} (Figure 8b). In RTA&DAAO, the diffusion and transferring of D-alanine and pyruvate are highly directional due to the shorter distance between the paired subunits of RTA^S and $DAAO^S$ (RTA^S-$DAAO^S$) as indicated in Figure 8a. Thus, forming the pyruvate→D-alanine→pyruvate cycles is highly efficient. The distance between the paired subunits of RTA^S and $DAAO^S$ (RTA^S=$DAAO^S$) in RTA#DAAO is larger than that in RTA&DAAO, and pyruvate and D-alanine are transferred between RTA^S and $DAAO^S$ by travelling a larger distance. It can be speculated that the transferring efficiency of pyruvate and D-alanine by RTA&DAAO is larger than that by RTA#DAAO. In addition, the BN-PAGE analysis (Figures 2 and 3) for RTA&DAAO and RTA#DAAO has provided the information of linking modes corresponding to the bands, the fraction of each band, and apparent molecular weight. Based on these information, the number of the key subunit RTA^S-$DAAO^S$ (paired subunits via a peptide bond) is 23.1% higher than that of the key subunit RTA^S=$DAAO^S$ (paired subunits via coiled-coil association). This implies that RTA&DAAO can generate more pyruvate→D-alanine→pyruvate cycles than

RTA#DAAO. Highly efficiently forming more pyruvate→D-alanine→pyruvate cycles contributes to the efficient utilization of pyruvate, this has a significant effect on the transamination reaction.

Conclusions

For enzymatic catalysis of transamination of amines, efficient utilization of the amino acceptor pyruvate can significantly contribute to the improvement of the transamination reaction. Three two-enzyme systems were studied to investigate how pyruvate can be used efficiently, including RTA&DAAO (via in vivo splicing of hetrosubunits, a covalent approach to linking hertrosubunits), RTA#DAAO (via association of hetrosubunits, a non-covalent approach to linking hertrosubunits), and RTA+DAAO (mixing two enzymes). For the system RTA+DAAO, there is no specific interaction between RTA and DAAO. The diffusion and transferring of D-alanine and pyruvate cannot be directional, and the pyruvate→D-alanine→pyruvate cycle cannot be formed for RTA+DAAO. In RTA&DAAO, the subunits of RTA^S were specifically ligated to the subunits of $DAAO^S$ in a one-by-one fashion, thus the heterosubunits are close to each other at a molecular distance. The diffusion and transferring of D-alanine and pyruvate between RTA and DAAO can be highly directional, and the pyruvate→D-alanine→pyruvate cycle can be formed highly efficiently. In RTA#DAAO, the subunits of RTA^S and $DAAO^S$ are paired through specific association. The transferring of pyruvate and D-alanine is directional. The distance between the paired subunits of RTA^S and $DAAO^S$ (RTA^S=$DAAO^S$) in RTA#DAAO is larger than that in RTA&DAAO, and pyruvate and D-alanine are transferred between RTA^S and $DAAO^S$ by travelling a larger distance. It can be speculated that the transferring efficiency of pyruvate and D-alanine by RTA&DAAO is larger than that by RTA#DAAO. The BN-PAGE analysis has demonstrated that the number of the key subunit RTA^S-$DAAO^S$ (paired subunits via a

peptide bond) in RTA&DAAO is 23.1% higher than that of the key subunit RTA^{S}=$DAAO^{S}$ (paired subunits via coiled-coil association) in RTA#DAAO. RTA&DAAO can generate more pyruvate→D-alanine→pyruvate cycles than RTA#DAAO. Highly efficiently forming more pyruvate→D-alanine→pyruvate cycles contributes to the efficient utilization of pyruvate, this has a significant promoting effect on the transamination reaction. For the transamination of amines, RTA&DAAO exhibited a higher catalysis efficiency than RTA#DAAO, and a much higher catalysis efficiency than the mixed enzymes RTA+DAAO.

Experimental section

Materials

DNA ligase, DNA polymerase, and restriction enzymes were purchased from New England Biolabs and Fermentas. Oligonucleotide primers were synthesized by BGI Tech. *Escherichia coli* strain DH5α was used as a host for DNA manipulation, and strain BL21 was used as a host for expressing enzymes. All other reagents were purchased from Sigma-Aldrich (Shanghai, China) and used without purification.

Construction of plasmids

Plasmid for the in vivo subunit splicing. Standard molecular cloning techniques were used for the construction of plasmids. The gene of D-amino acid oxidase (DAAO) was amplified by PCR using the paired primers DAAO-fp and DAAO-rp (supplementary Table S1), and the genomic DNA of *Trigonopsis variabilis* was used as template. A DNA extraction kit (Omega Bio-tek) was used to purify the DAAO gene. The purified DAAO gene was digested with both NdeI and KpnI restriction endonucleases, and then was ligated into the plasmid pETDuet-1 that had been cleaved with NdeI and KpnI restriction endonucleases. The expression plasmid DAAO-pETDuet in *Escherichia coli* was constructed, comprising an N-terminal hexahistidine tag. The Int^{C}-link gene was

amplified by PCR using the Int^C-fp and Int^C-rp primers (supplementary Table S3). The purified Int^C-link gene was digested with KpnI and XhoI restriction endonucleases, then was ligated into the vector DAAO-pETDuet that had been cleaved with KpnI and XhoI restriction endonucleases. The constructed expression plasmid was designated as DAAO-limk-Int^C-pETDuet.

R-ω-transaminase (RTA) gene was synthesized and cloned in pUC57 plasmid by Genewiz (Suzhou, China). The RTA gene was amplified by PCR using primers RTA-fp and RTA-rp (supplementary Table S3). The purified RTA gene was digested with both BamHI and HindIII restriction endonucleases, and then was ligated into the plasmid DAAO-limk-Int^N-pETDuet, which had been cleaved with BamHI and HindIII restriction endonucleases. Thus, the vector DAAO-limk-Int^N/RTA-pETDuet in *Escherichia coli* was constructed. The gene of Int^C-link was amplified by PCR using the Int^C-fp and Int^C-rp primers (supplementary Table S3). The purified Int^C-link gene was digested with both BamHI and NcoI restriction endonucleases, and then was ligated into the plasmid DAAO-limk-Int^N/RTA-pETDuet, which had been cleaved with BamHI and NcoI restriction endonucleases. The expression plasmid DAAO-link-Int^N/Int^C-link-RTA-pETDuet was finally constructed as illustrated in supplementary Figure S1, which was confirmed by sequence analysis. For expressing RTA, the vector RTA-pET28a was constructed comprising a C-terminal hexahistidine tag.

Plasmids for the fusions of Z_R to RTA and Z_E to DAAO. The gene of DAAO was amplified by PCR using the paired primers DAAO-ffp and DAAO-rfp (supplementary Table S4). The purified DAAO gene was digested with both NdeI and XhoI restriction endonucleases, and then was ligated into the plasmid pET28 that had been cleaved with NdeI and XhoI restriction endonucleases. The gene of the Link-C_R-C_E-Link peptide (supplementary Table S5) was synthesized by BGI (Shenzhen, China). The gene of

Link-CR-CE-Link was digested with both NcoI and NheI restriction endonucleases, and then was ligated into the plasmid DAAO-pET28 that had been cleaved with NcoI and NheI restriction endonucleases. Thus the plasmid CE-DAAO-pET28 was constructed (supplementary Figure S4a).

The RTA gene was amplified by PCR using primers RTA-ffp and RTA-rrp (supplementary Table S4). The purified RTA gene was digested with both NheI and BamHI restriction endonucleases, and then was ligated into the plasmid pET28, which had been cleaved with NheI and BamHI restriction endonucleases. The gene of Link-CR-CE-Link was digested with both SacI and XhoI restriction endonucleases, and then was ligated into the plasmid RTA-pET28 that had been cleaved with SacI and XhoI restriction endonucleases. Thus the plasmid CR-RTA-pET28 was constructed (supplementary Figure S4b).

Enzyme expression and in vivo subunit splicing

Escherichia coli BL21 cells harboring various plasmids grew in Luria-Bertani medium with 50 μg/ml Amp at 37 °C. When reaching an OD_{600} of 0.5, the cells were induced with 0.2 mM isopropyl β-D-1-thiogalactopyranoside (IPTG), and an additional 8 h was required for expressing enzymes at 25°C for coexpressing the precursors Int^C-link-RTA and DAAO-link-Int^N and the *in vivo* splicing. The *Escherichia coli* cells were harvested by centrifuging at 6000 g at 4°C for 30 min. The cells were then lysed under ultrasonication on ice, and cell debris was removed by centrifugation of the lysate at 8,000 *g* at 4 °C for 30 min. The supernatant was transferred to a fresh tube. The enzymes were purified using Ni Sepharose beads (GE Life Sciences) in a chromatography column (GE Life Sciences) with 500 mM imidazole as the elution liquid. The imidazole was then removed from the purified enzymes by dialysis into a buffer (500 mM NaCl, 50 mM Tris-Cl pH 7.5, 1 mM EDTA). The purified enzyme comprising the splicing

product RTA&DAAO was further fractionated by ultrafiltration (GE Healthcare, 50 KDa cut off). The fusion enzymes Z_R-RTA and Z_E-DAAO were expressed similarly and purified using Ni Sepharose beads.

Blue native PAGE

Blue native PAGE (BN-PAGE) was performed at room temperature using 3.5% stacking gel and 4–12% separating gel with the gel dimensions 0.15×10×10 cm.[23] The gel compositions and the cathode and anode buffers were prepared according to the paper.[24] Prior to use, the buffers were stored at 4 °C. The marker protein standard (Invitrogen) consisted of seven protein components with molecular weights from 66~1236 kDa. 2 μg enzyme sample was added to each lane with an enzyme concentration of 0.5 mg/mL. The BN-PAGE electrophoresis was initially performed at 100 V. After enzyme reaching the separating gel, the voltage was changed to 160 V and run until the enzyme front reached the end of the gel. Once the blue running front was moved about one-third to half of the separating gel, the buffer was changed to a low concentration.

The obtained gels were scanned and high resolution images (600 dpi) were obtained. The gel images were processed using Adobe Photoshop CS6 (version 13) to obtain the best contrast for densitometry analysis. The Gel-Pro Analyzer software program was used to estimate optical densitometry for determining relative abundances of the RTA&DAAO fractions. By comparing the electrophoretic mobility of the enzyme fractions with that of Marker proteins, the apparent molecular weights of the RTA&DAAO fractions were determined. The relative mobility was determined by measuring the distance from the top of the gel to the middle of the dye front, and dividing the second measurement by the first. The relative mobility versus molecular weight for the Marker proteins is shown in supplementary Figure S3. The curve was

used as a standard curve for determination of the apparent molecular weights of the RTA&DAAO fractions.

Circular dichroism (CD) spectra

The change of secondary structures of the enzymes was monitored by measuring CD spectra on a JASCO J-810 CD instrument. The scanning was performed at 30 °C with a scan rate of 100 nm/min with a bandwidth of 1.0 nm. Cell length was 1 cm, and the enzyme concentration was 0.2 mg/mL. All the samples were prepared by dissolution of the enzymes in PBS buffer. The CD spectrum of the PBS buffer was measured and used as control. Averaged spectra were obtained by repeating five times scan.

Fluorescence measurements

Two buffers were first prepared, buffer A (pH 7.5) consisting of 50 mM potassium phosphate and 2 mM EDTA, and buffer B (pH 7.5) comprising 50 mM potassium phosphate, 2 mM EDTA, and 4 M urea. The enzyme solutions were diluted into buffer A and buffer B to prepare samples, incubated at 4 ^{0}C overnight, with a final enzyme concentration of 2.0 μmol/L each. Buffer A was used to prepare acrylamide solutions with different concentrations. Fluorescence spectra were measured on a spectrophotometer (F-7000), a 1 cm pathlength cuvette was used. Emission spectra of the tryptophan were recorded for wavelength ranging from 300 to 400 nm, using an excitation wavelength of 295 nm. The slits for excitation and emission were set at 5 nm, the scan speed was 1200 nm/min. For all the samples, the background fluorescence was subscribed to correct the fluorescence spectra. A baseline control was realized for each experiment. The experiments for fluorescent quenching were performed by addition of the acrylamide solutions. A aliquot of acrylamide solution was added to the samples (2 mL), incubation of the solutions was carried out for 6 min prior to recording the emission spectra.

Enzymatic activity

For transformation of the amines, the enzymatic catalysis was performed at 30 °C. The enzyme concentrations were: 0.2 mg/mL RTA&DAAO; 0.089 mg/mL RTA-Z_R+ 0.111 mg/mL DAAO-Z_E; 0.088 mg/ml RTA+0.112 mg/ml DAAO. For the catalysis by RTA&DAAO and RTA+DAAO, the substrate solutions were prepared by dissolving amine (5 mM), pyridoxal-5'- phosphate (1 mM), and sodium pyruvate (0.5 mM) in Tris-HCl (100 mM, pH 8.5). For the catalysis by RTA#DAAO, the substrate solutions were prepared by dissolving amine (5 mM), pyridoxal-5'- phosphate (1 mM), and sodium pyruvate (0.5 mM) in KPOi (100 mM, pH 7.5). Enzyme concentrations were determined by the bicinchoninic acid assay. Amines were quantified by HPLC using a C18 column (Diamonsil). The mobile phase was acetonitrile/acidic acid/water (60:0.1:39.9 by vol) at 0.8/1.0 ml/min. The injection was 20 ul.

Acknowledgments

This work was supported by The National Science Foundation of China (21576018, 21776011).

References

[1] A. Nobili, F. Steffen-Munsberg, H. Kohls, I. Trentin, C. Schulzke, M. Höhne, U. T. Bornscheuer. *ChemCatChem,* 2015,7,757-760

[2] E. O'Reilly, C. Iglesias, N. J. Turner. *ChemCatChem*, 2014, 6, 992-995.

[3] D. Monti, M. C. Forchin, M. Crotti, F. Parmeggiani, F. G. Gatti, E. Brenna, S. Riva. *ChemCatChem*, 2015, 7,3106-3109

[4] A. Łyskowski, C. Gruber, G. Steinkellner, M. Schürmann, H. Schwab, K. Gruber, K. Steiner, *PLoS. One.* **2014**, *9*, e87350.

[5] E. S. Park, M. Kim, J. S. Shin, *Appl. Microbiol. Biotechnol.* **2012**, *93*, 2425-2435.

[6] D. Koszelewski, D. Clay, D. Rozzell, W. Kroutil, *Eur. J. Org. Chem.* **2009**, 2289–2292.

[7] J. Jiang, X. Chen, D. Zhang, Q. Wu, D. Zhu, *Appl. Microbiol. Biotechnol.* **2015**, *99*, 2613-2621.

[8] H. Yun, B. Y. Hwang, J. H. Lee, B. G. Kim, *Appl. Environ. Microbiol.* **2005**, *71*, 4220.

[9] L. Pollegioni, G. Molla, *Trends. Biotechnol.* **2011**, *29*, 276-283.

[10] M. D. Truppo, N. J. Turner, J. D. Rozzell, *Chem. Commun.* **2009**, *16*, 2127.

[11] C. Lindbladh, M. Rault, C. Hagglund, W. C. Small, K. Mosbach, L. Bülow, C. Evans, P. A. Srere, *J. Biochem.* **1994**, *33*, 11692-11698.

[12] K. Du, J. J Zhao, J. Sun, W. Feng, *Bioconjugate Chem.* **2017**, *28*, 1166−1175.

[13] R. Li, X. Zhou, D. Liu, W. Feng. *Free Radical* Bio. Med., 2018, 129, 38-145.

[14] N. H. Shah, V. P. Miquel, T. W. Muir, *Angew. Chem. Int. Edit.* **2011**, *50*, 6511-6515.

[15] W. M. Park, J. A. Champion, *Angew. Chem. Int. Edit.* **2013**, *52*, 8098-8101.

[16] N. Wiedemann, V. Kozjak, A. Chacinska, B. Schönfisch, S. Rospert, M. T. Ryan, N. Pfanner, C. Meisinger, *Nature*. **2003**, *424*, 565-571.

[17] R. W. Lencki, J. Arul, R. J. Neufeld, *Biotechnol. Bioeng.* **1992**, *40*, 1427–34.

[18] A. K. Kumar, P. Goswami, *J. Biochem.* **2009**, *145*, 259-65.

[19] L. R. Fernandez, *Enzym. Microb. Technol.* **2009**, *45*, 405-418.

[20] D. Georlette, V. Blaise, F. Bouillenne, B. Damien, S. H. Thorbjarnardóttir, E. Depiereux, C. Gerday, V. N. Uversky, G. Feller, *Biophys. J.* **2004**, *86*, 1089-1104.

[21] O. L. Brady, G. V. Elsmie, *Analyst.* **1926**, *51*, 77-78.

[22] A. C. Reyes, T. L. Amyes, J. P. Richard, *J. Am. Chem. Soc.* **2017**, 139 (45): 16048–16051.

10.1002/cbic.201800646

[23] A. B. Nowakowski, W. J. Wobig, D. H. Petering, *Metallomics.* **2014**, *6*, 1068-1078.

[24] W. Ilka, P. B. Hans, S. Hermann, *Nature Protocols.* **2016**, *1*, 418–428.

10.1002/cbic.201800646

Figures

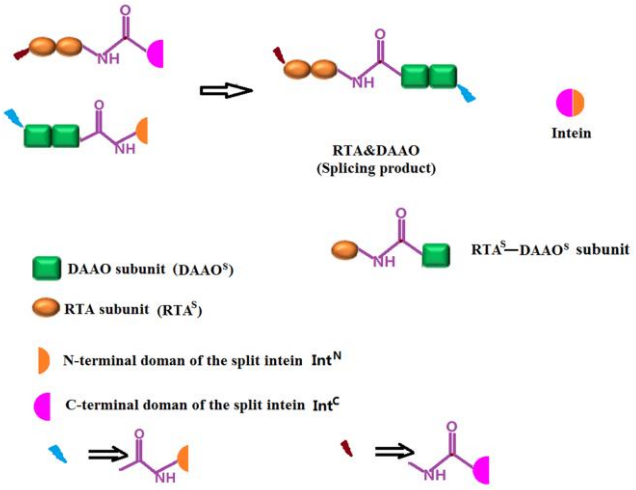

Figure 1. Schematic presentation of subunit splicing for the ligation of the RTA and DAAO subunits with peptide bond.
Through the intein-mediated subunit splicing, the N-terminus of the RTA subunit is specifically ligated to the C-terminus of the DAAO subunit with native peptides. In the splicing product (RTA&DAAO), the RTA^S–DAAO^S subunit is the key subunit. The DAAO and RTA subunits, that are not involved in the subunit splicing reaction, are associated with the RTA^S–DAAO^S subunit.

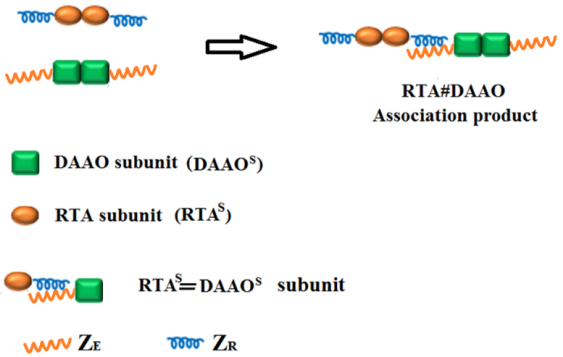

Figure 2. Schematic presentation for establishing two-enzyme system RTA#DAAO through coiled-coil association of Z_E and Z_R in vitro.
In the association product (RTA#DAAO), the RTA^S=DAAO^S subunit is the key subunit.
Z_R: arginine-rich leucine zipper; Z_E: glutamic acid-rich leucine zipper

10.1002/cbic.201800646

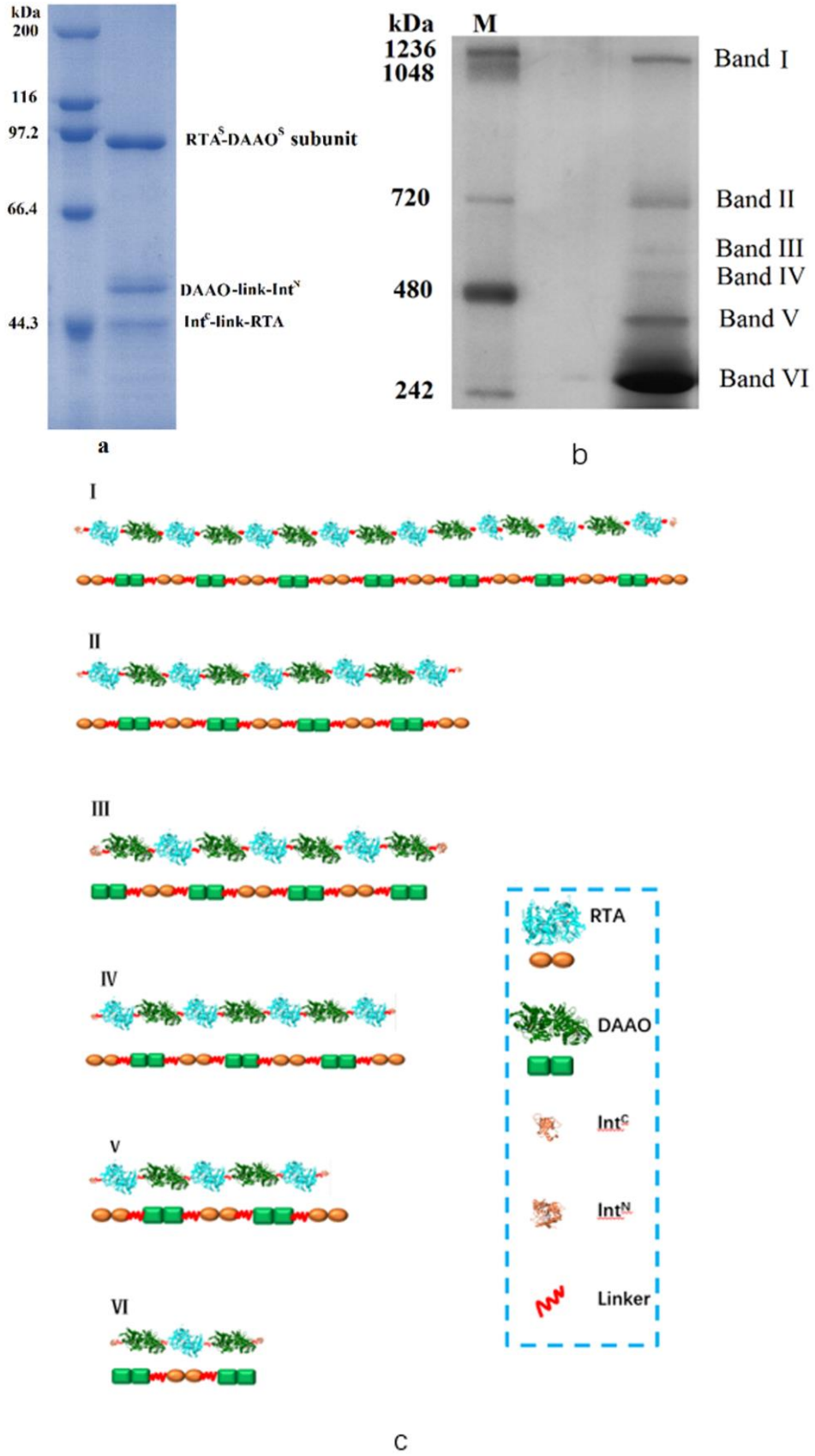

Figure 3. (a) Analysis of the splicing product RTA&DAAO by SDS-PAGE.
(b) Analysis of the splicing product RTA&DAAO by BN-PAGE.
Lane M: marker.
(c) Schematic diagram representing the RTA&DAAO fractions resulted from the

ligation modes of
RTA~DAAO~RTA~DAAO~RTA~DAAO~RTA~DAAO~RTA~DAAO~RTA~DAAO~RTA~DAAO~RTA (band I); RTA~DAAO~RTA~DAAO~RTA~DAAO~RTA~DAAO~RTA (band II); DAAO~RTA~DAAO~RTA~ DAAO~RTA~DAAO (band III); RTA~DAAO~RTA~DAAO~RTA~DAAO~RTA (band IV); RTA~DAAO~RTA~DAAO~RTA (band V); DAAO~RTA~DAAO (band VI).

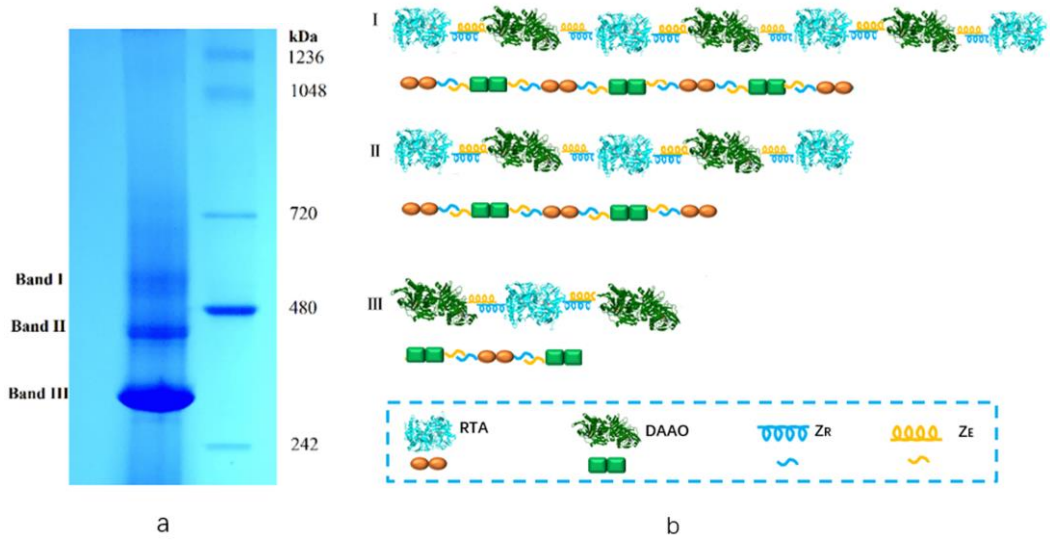

Figure 4. (a) Analysis of the association product RTA#DAAO by BN-PAGE. (b) Schematic diagram representing the RTA#DAAO fractions resulted from the association modes of
RTA≈DAAO≈RTA≈DAAO≈RTA≈DAAO≈RTA (band I);
RTA≈DAAO≈RTA≈DAAO≈RTA (band II);
DAAO≈RTA≈DAAO (band III).

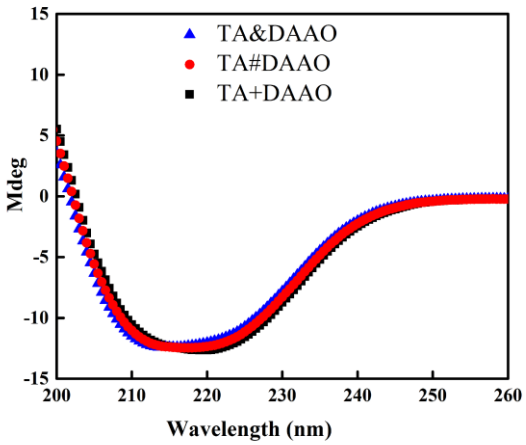

Figure 5. CD spectra for the splicing product RTA&DAAO, association product RTA#DAAO, and mixed enzymes RTA+DAAO.

10.1002/cbic.201800646

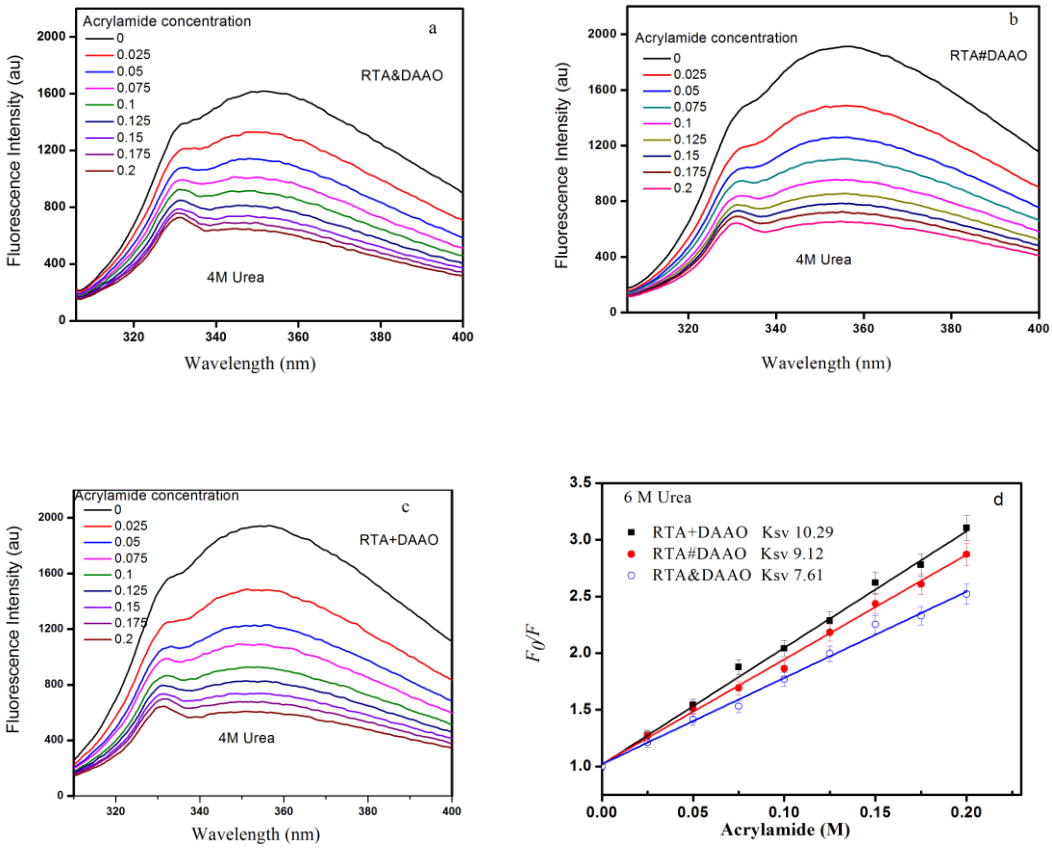

Figure 6. (a, b, c) Change of fluorescence intensity of the two-enzyme systems with acrylamide concentration (M). (d) Stern-Volmer plots for the quenching of protein fluorescence with acrylamide. F_0 and F are the fluorescence intensities in absence and presence of acrylamide, respectively.

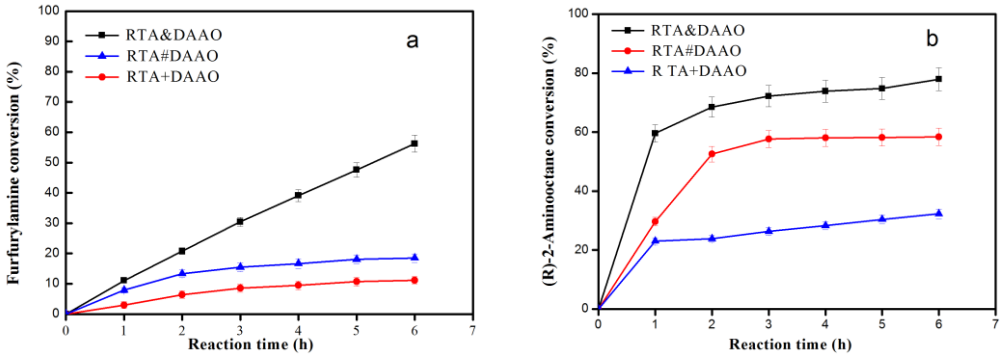

10.1002/cbic.201800646

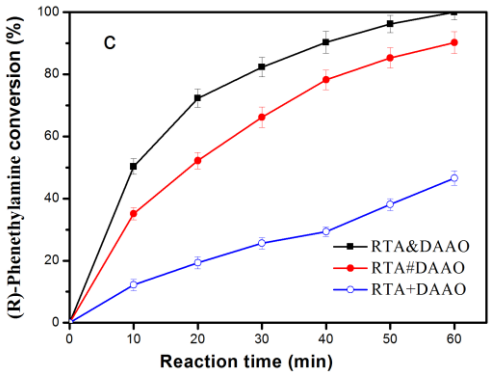

Figure 7. Conversion of (R)-amines under the catalysis of two-enzyme systems
Substrates: (a) Furfurylamine; (b) (R)-1-Aminoindan; (c) (R)-Phenethylamine
For catalyzing the transamination reactions, equal molar ratio of RTA to DAAO was adopted for the two-enzyme system RTA&DAAO, RTA#DAAO, and RTA+DAAO (see experimental section).
The concentrations of amines were 5 mM, and the concentration of pyruvate was 0.5 mM.
For RTA&DAAO, the mixture of bands I~VI was used. For RTA#DAAO, the mixture of the mixture of band I~III was used.

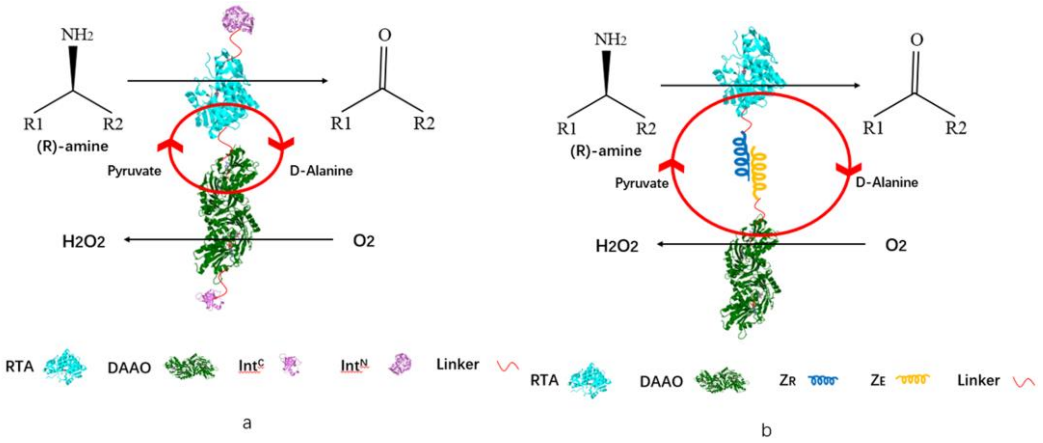

Figure 8. Schematic presentation for the coordination of RTA and DAAO by the two-enzyme systems. (a) RTA&DAAO; (b) RTA#DAAO

10.1002/cbic.201800646

Table of contents text

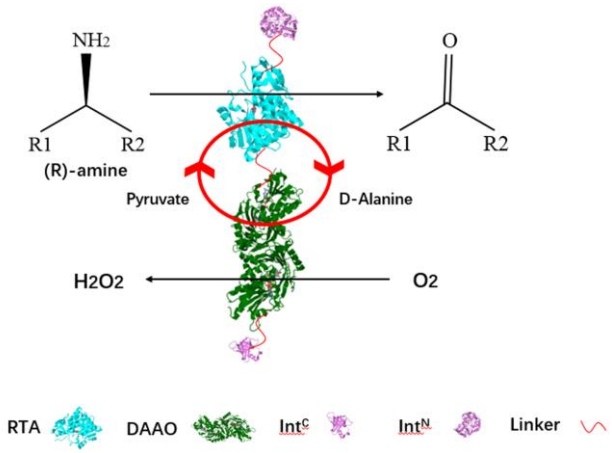

The N-terminus of the subunit of *R*-ω-transaminase is specifically ligated to the C-terminus of the subunit of D-amino acid oxidase with native peptides. The hetrosubunits are spatially arranged in a one-by-one fashion at a molecular distance. The pyruvate→D-alanine→pyruvate cycles are efficiently formed, promoting the transamination reaction forward.